DEVELOPING LAMINAR MIXED CONVECTION HEAT TRANSFER THROUGH VERTICAL CONCENTRIC ANNULI WITH ADIABATIC INNER CYLINDER

Prof. Dr. Ihsan Y. Hussain **Dr. Akeel Abdullah Mohammed** **Ghada A. Sadiq**
Baghdad University **University of Technology** **Al-Mustansiriya University**
Mech. Eng. Dep. **Mech. Eng. Dep.** **Mech. Eng. Dep.**

ABSTRACT

Theoretical and experimental investigations have been carried out on developing laminar combined free and forced convection heat transfer in a vertical concentric annulus with uniformly heated outer cylinder (constant heat flux) and adiabatic inner cylinder for both aiding and opposing flows. The theoretical investigation involved a mathematical modeling and numerical solution for two dimensional, symmetric, simultaneously developing laminar air flows was achieved. The governing equations of motion (continuity, momentum and energy) are solved by using implicit finite difference method and the Gauss elimination technique. The theoretical work covers heat flux range from (200 to 1500) W/m^2, Re range from 400 to 2000 and ($1.36\times10^5 \le Ra \le 1.1\times10^7$) with radius ratio of 0.555 which is the same radius ratio used in the experimental part of this study and Pr=0.7. The experimental work includes construct a rig consists essentially of an annulus with uniformly heated outer cylinder and adiabatic inner cylinder to give clear insight into heat transfer process and compare its results with that obtained in theoretical part, the range of the study are (Re= 383, 724, 1000, 1500) and heat flux equal to (q =370, 422, 588, 980) W/m^2. Numerical results were represented by the temperature profile, axial velocity profile, outer surface temperature and the distribution of local Nusselt number along the dimensionless axial distance. The velocity and temperature profile results have revealed that the secondary flow created by natural convection have significant effects on the heat transfer process. Results reveal also that the experimental local Nusselt number along the annulus follows the same trend as present theoretical results with mean difference 10.23 %.

الخلاصة:

أجريتْ دراسة نظرية وعملية لانتقال الحرارة بالحمل المختلط لجريان الهواء المتطور الطباقي خلال تجويف حلقي عمودي ذو أسطوانتين متمركزتين؛ الخارجية مسخنة تسخين منتظم (فيض حراري ثابت) و الداخلية معزولة (لكلا الجريانين المساعد والمعاكس). البحث النظري تضمن عمل نموذج رياضي و دراسة عددية لجريان الهواء الطباقي المشكل تراكبيا ثنائي البعد. تم حل المعادلات الحاكمة للحركة (الاستمرارية ، الزخم ، الطاقة) باستخدام طريقة الفروقات المحددة و طريقة معكوس المصفوفة (طريقة كاوس). غطت الدراسة النظرية فيضا حراريا مداه من ٢٠٠ واط\م^2 إلى 1500واط\م^2 ، معدل رقم رينولدز Re من ٤٠٠ إلى ٢٠٠٠ و ($1.36\times10^5 \le Ra \le 1.1\times10^7$) مع نسبة نصف قطر تساوي ٠,٥٥٥ وهي نفسها المستخدمة في الجزء العملي من هذا البحث ورقم براندتل Pr =0.7. اشتمل الجزء العملي بناء جهاز تجريبي يتكون من تجويف حلقي متمركز بأسطوانة خارجية مسخنة تسخين منتظم و أسطوانة داخلية معزولة لاعطاء نظرة واضحة لعملية انتقال الحرارة ومقارنة نتائجها مع تلك التي تم الحصول عليها في الجزء النظري مدى الدراسة (Re= 383, 724, 1000, 1500) والفيض الحراري مساوي الى (q =370, 422, 588, 980) W/m^2 . تم تمثيل النتائج النظرية برسم توزيع درجة الحرارة، توزيع السرعة المحورية على طول التجويف الحلقي، درجة حرارة الاسطوانة الخارجية و توزيع رقم نسلت الموقعي مع المسافة المحورية اللابعدية. اظهرت نتائج توزيع السرعة و درجات الحرارة ان الجريان الثانوي الناتج من الحمل الحر(الطبيعي) له تاثير مهم على عملية انتقال الحراة. النتائج بينت بان قيم رقم نسلت الموقعي العملية تتخذ نفس سلوك قيم رقم نسلت الموقعي النظرية لكن أعلى تقريباً مع معدل فرق 10.23 %.

KEYWORDS: **Combined Convection, Concentric Annulus, Numerical and Experimental.**

INTRODUCTION

The convective heat transfer is of great importance in many engineering applications. A number of investigations have been carried out to study pure forced convection and pure natural convection in different geometries. However, mixed convection, i.e., combined free and forced convection is the most general single phase heat transfer phenomenon and has received considerable attention in recent years. Such a process occurs when the effect of the buoyancy force in forced convection or the effect of forced flow in free convection becomes significant. In mixed convection flows, the forced convection effects and the free convection effects may be of comparable magnitudes.

Mixed convection processes may be divided into external flows over immersed bodies, free boundary flows, and internal flows. In internal flows, mixed convective flows are quite common and there can be a variety of geometries, such as cylindrical, rectangular and triangular cross- sections. The concentric annular duct is of technical importance, as it represents numerous heat transfers and fluid flow devices. Mixed convection in concentric cylinders has been the subject of many investigations for quite some time, for example: Gas- cooled electrical cables, heat exchanger designed for chemical processes require the consideration of mixed convection in an annular flow, cooling of nuclear fuel rods where the results for the buoyancy-influenced convection in an annulus are useful and the collection of solar energy**.**

(El-Sharrawi and Sarhan 1980) studied mixed convection of upward and downward air flow in an annulus of radius ratio (0.5, 0.8, and 0.9) and Pr = 0.7. The flow with a flat velocity profile at the entrance was considered. The thermal boundary conditions of one wall being isothermal and other adiabatic. They noticed that when the free convection opposes the forced flow (heating with down flow or cooling with up flow) there exists a possibility of flow reversal near the heated boundary while such a flow reversal may occur near the insulated wall if the free convection is aiding the force flow. The axial velocity profiles development, pressure drop, mixing cup temperature and heat transfer coefficient along the annulus were calculated.

(Hashimoto et. al 1986) performed a numerical investigation of the mixed convection (both upward and downward helium gas flow with Pr = 0.671), with a simultaneously developing hydrodynamic and thermal boundary layer in a vertical annulus of (0.9) radius ratio. The flow was considered under isothermal or constant heat flux inner wall and adiabatic outer wall. The equations of the continuity, momentum, energy, and integral continuity were solved on the basis of the boundary layer approximation. The critical conditions effect on the flow which create a reversal flow and the effect of property variations on both Nusselt number and friction factor were obtained.

(Hanzawa et. al 1986) performed experiments to study the mixed convection of upward gas flow in vertical annulus of radius ratio range from (0.29 to 0.63) and hydraulic diameter to heating section length range from (0.34 to 1.4). A part of the inner tube was isothermally heated while the outer tube was kept adiabatic. The study covered Gr range from (1.5×10^6 to 2×10^8), Re range from (20 to 1000). The effects of operating conditions on the temperature profiles, flow pattern and heat transfer coefficient were investigated.

Numerical solutions for the problem of steady state laminar combined convection flows in vertical annular ducts were presented by **(Heggs et. al 1988)**. The axial diffusion terms were assumed to be negligible in the governing equations and the resulting parabolic equations were solved by using an implicit finite difference scheme and a marching solution technique. Constant wall temperature boundary conditions were used and investigations were restricted to the case Pr =0.72. Large ranges of values of the governing parameters Gr/Re and radius ratio were considered ($-90 \leq Gr/Re \leq 125$) and ($0.1 \leq N \leq 0.99$). For large values of the ratio

Gr/Re reverse flow was present in the fluid. A modified solution technique was used throughout the region of the annulus containing the flow reversal and complete solutions were presented for these situations for the first time. Heat transfer data in the form of flow average temperatures and local Nusselt numbers at both the inner and outer walls were presented. It was found that the behavior of the local Nusselt number on each wall was considerably different.

The laminar mixed convection in vertical channels was studied numerically by using an implicit finite difference method by **(Shaik 2005**) emphasis was devoted to analyze the hydrodynamic behavior of mixed convection flow under isothermal boundary conditions regarding. The pressure and pressure gradient variation along the channel (from the entrance till the fully developed region) was obtained numerically. Moreover, critical values of the buoyancy parameter Gr/Re were determined and the radius ratio (0.1, 0.3, 0.5 and 0.7). The hydrodynamic and heat transfer parameters of relevant importance were also presented.

The present work in its theoretical part includes a finite difference method using mesh grid point for vertical annulus mixed convection, the range of the work are ($400 \le Re \le 2000$),($1.36\times10^5 \le Ra \le 1.1\times10^7$) and the heat flux for aiding and opposing flow (200 to 1500) W/m^2 of radius ratio (0.555). The experimental investigation is made for simultaneously developing mixed convection laminar air flow in a vertical annulus of radius ratio (0.555) and with uniformly heated outer cylinder and adiabatic inner cylinder. The range of the work are (Re= 383, 724, 1000, 1500) and heat flux equal to (q =370, 422, 588, 980) W/m^2 with radius ratio (N=0.555).

MATHIMATICAL MODELING

The present analysis assumes incompressible fluid, steady state laminar air flow with two dimensional in the axial and radial directions for hydrodynamically and thermally developing flow see **Fig.1**. The assumptions were used are negligible viscous dissipation, no internal heat generation and heat dissipation, Cp and K are constants and the density ρ in the buoyancy term and the viscosity μ are varying with temperature in a quadratic equation. The governing equations become **(Kayes 1966)**:

$$\frac{\partial u}{\partial z}+\frac{v}{r}+\frac{\partial v}{\partial r}=0 \tag{1}$$

$$\rho_l\cdot\left(v\frac{\partial u}{\partial r}+u\frac{\partial u}{\partial z}\right)=-\frac{\partial p}{\partial z}\pm\rho g+\mu\cdot\left(\frac{\partial^2 u}{\partial z^2}+\frac{1}{r}\frac{\partial u}{\partial r}+\frac{\partial^2 u}{\partial r^2}\right)+2\left(\frac{\partial \mu}{\partial z}\cdot\frac{\partial u}{\partial z}\right)+\frac{\partial \mu}{\partial r}\cdot\left(\frac{\partial v}{\partial z}+\frac{\partial u}{\partial r}\right) \tag{2}$$

The sign ± ρg in the buoyancy term refers to downward or upward flow respectively.

$$\rho_l\cdot\left(v\frac{\partial v}{\partial r}+u\frac{\partial v}{\partial z}\right)=-\frac{\partial p}{\partial r}+\mu\cdot\left(\frac{\partial^2 v}{\partial z^2}+\frac{1}{r}\frac{\partial v}{\partial r}-\frac{v}{r^2}+\frac{\partial^2 v}{\partial r^2}\right)+2\cdot\left(\frac{\partial \mu}{\partial r}\cdot\frac{\partial v}{\partial r}\right)+\frac{\partial \mu}{\partial z}\cdot\left(\frac{\partial v}{\partial z}+\frac{\partial u}{\partial r}\right) \tag{3}$$

$$\left(v\frac{\partial t}{\partial r}+u\frac{\partial t}{\partial z}\right)=\frac{k}{\rho_i\cdot Cp}\cdot\left(\frac{\partial^2 t}{\partial z^2}+\frac{1}{r}\frac{\partial t}{\partial r}+\frac{\partial^2 t}{\partial r^2}\right) \tag{4}$$

The conversation of mass (continuity equation) can be expressed in the following integral form:

$$\rho_i\cdot\pi\cdot\left(r_o^{\,2}-r_i^{\,2}\right)\cdot u_i=\int_{r_i}^{r_o}2\pi\cdot r\cdot\rho\cdot u\cdot dr \tag{5}$$

The dynamic viscosity μ and density ρ are considered to be dependent on temperature according to the following relations **(Collins 1971);**

$$\mu = \mu_i\left(C_1 + C_2 t - C_3 t^2\right) \tag{6}$$

$$\rho = \rho_i\left(C_4 - C_5 t + C_6 t^2\right) \tag{7}$$

Dimensionless Equations

The physical properties, equations in dimensionless form become:

$$\mu = \mu_i\left(Co_1 + Co_2 T + Co_3 T^2\right) \tag{8}$$

$$\rho = \rho_i\left(Co_4 + Co_5 T/G + Co_6 T^2/G\right) \tag{9}$$

where

$Co_1 = C_1 + C_2 t_i - C_3 t_i^2$,
$Co_2 = (1/G.C_5)(C_2 - 2C_3 t_i)$
$Co_3 = -C_3/G^2 C_5^2$,
$Co_4 = C_4 - C_5 t_i + C_6 t_i^2$
$Co_5 = (2C_6 t_i/C_5) - 1$,
$Co_6 = C_6/G C_5^2$

$$\frac{\partial U}{\partial Z} + \frac{V}{R} + \frac{\partial V}{\partial R} = 0 \tag{10}$$

$$V\frac{\partial U}{\partial R} + U\frac{\partial U}{\partial Z} = -\frac{\partial P}{\partial Z} \pm \frac{4(1-N)^2}{Re^2}\left[G Co_4 + T(Co_5 + Co_6 T)\right] + \frac{2(1-N)}{Re}\left[\left\{Co_1 + T(Co_2 + Co_3 T)\right\}\cdot\left(\frac{\partial^2 U}{\partial Z^2} + \frac{1}{R}\cdot\frac{\partial U}{\partial R} + \frac{\partial^2 U}{\partial R^2}\right)\right] + \frac{2(1-N)}{Re}\left[\left\{Co_2 + 2TCo_3\right\}\left(2\frac{\partial T}{\partial Z}\cdot\frac{\partial U}{\partial Z} + \frac{\partial T}{\partial R}\left\{\frac{\partial V}{\partial Z} + \frac{\partial U}{\partial R}\right\}\right)\right] \tag{11}$$

$$V\frac{\partial V}{\partial R} + U\frac{\partial V}{\partial Z} = -\frac{\partial P}{\partial R} + \frac{2(1-N)}{Re}\cdot\left\{Co_1 + T(Co_2 + Co_3 T)\right\}\cdot\left(\frac{\partial^2 V}{\partial Z^2} + \frac{1}{R}\frac{\partial V}{\partial R} - \frac{V}{R^2} + \frac{\partial^2 V}{\partial R^2}\right) + \frac{2(1-N)}{Re}\cdot\left\{Co_2 + 2TCo_3\right\}\cdot\left(2\frac{\partial T}{\partial R}\cdot\frac{\partial V}{\partial R} + \frac{\partial T}{\partial Z}\left\{\frac{\partial V}{\partial Z} + \frac{\partial U}{\partial R}\right\}\right) \tag{12}$$

$$V\frac{\partial T}{\partial R} + U\frac{\partial T}{\partial Z} = \frac{2(1-N)}{Re\,Pr}\cdot\left(\frac{\partial^2 T}{\partial Z^2} + \frac{1}{R}\frac{\partial T}{\partial R} + \frac{\partial^2 T}{\partial R^2}\right) \tag{13}$$

$$\frac{1}{2}\cdot\left(1 - N^2\right) = \int_N^1 U\cdot R\cdot\left(Co_4 + Co_5\cdot T/G + Co_6\cdot T^2/G\right)\cdot dR \tag{14}$$

Boundary conditions in dimensionless form:

Entry condition

$$U = 1\ ,\ V = 0\ ,\ P = 0\ ,\ T = 0$$

Outer wall thermal condition

$$q = \left(k\cdot\frac{\partial t}{\partial r}\right)_{r=r_o} = \left(k\cdot\frac{\partial\left(T/G\cdot C_5 + t_i\right)}{\partial\left(R\cdot r_o\right)}\right)_{R=1}$$

$$\left(\frac{\partial T}{\partial R}\right)_{R=1} = \frac{q.r_o^4.g\cdot C_5}{k\cdot\nu_i^2}$$

Wall flow conditions

at R = N , U = 0 , V = 0 for all z
at R = 1 , U = 0 , V = 0 for all z

NUMERICAL SOLUTION

The numerical approximation method used is finite difference in the differential equations. The energy equation will be solved by a direct implicit method and the hydrodynamic part of the problem will be solved by means of an extension to the linearized implicit finite difference technique.

In the thermal length, problem of air flow with constant physical properties except the density in the buoyancy term is that the energy equation (11) is not couple with the equations of conservation of mass and momentum (8-10). This leads to special treatment for this problem by dividing it into two parts; the equation of energy can be solved to determine the temperature profile after which the equation of conversation of mass and momentum can be solved to determine the hydrodynamic characteristics of entry length using the temperature profiles previously obtained from the thermal calculations. Equation for temperature was written for each radial position at first axial step. This gives a set of M-1 equations for unknowns T's that were solved by Gauss elimination method. A rectangular grid was used with suffices m and n for the radial and axial directions, respectively. A uniform radial spacing was used, but the axial step size could be varied by doubling it at arbitrary axial locations. Basically, finite difference methods are used to give sets of linear equations for the variables U, V, P and T at the unknown axial position ("n+1"). Where the product of the two unknowns occurs, linearity is achieved by putting one unknown at its value of the previous known step ("n").

Numerical formulation

Continuity equation

$$\left(\frac{S\cdot x}{x-1}\right)V_{n+1,m}-S\cdot V_{n+1,m-1}+\frac{1}{2\Delta Z}U_{n+1,m}+\frac{1}{2\Delta Z}U_{n+1,m-1}=\frac{1}{2\Delta Z}\left(U_{n,m}+U_{n,m-1}\right) \quad (15)$$

$$R=\frac{x-1}{S}\quad,\quad x=F+m\quad,\quad N=\frac{F}{S}$$

F = number of the node at the inner surface from the center.

S = total radial mesh point from the center (S = F + M).

Momentum equations in axial and radial directions respectively:

$$\left[\frac{S^2(1-N)}{Re}\left\{T_A\frac{(2x-1)}{(x-1)}+\frac{T_B}{2}(T_{n+1,m+1}-T_{n+1,m-1})\right\}-\frac{S}{2}\cdot V_{n,m}\right]*(U_{n+1,m+1})+\left[\frac{2(1-N)}{Re}\cdot\left\{T_A\left(\frac{1}{\Delta Z^2}-2S^2\right)\right\}\right]*(U_{n+1,m})+\left[\frac{2(1-N)}{Re}\left\{\frac{2T_B}{\Delta Z^2}\cdot(T_{n+1,m}-T_{n,m})\right\}-\frac{U_{n,m}}{\Delta Z}\right]*(U_{n+1,m})+\left[\frac{S^2(1-N)}{Re}\left\{T_A\frac{(2x-3)}{(x-1)}-\frac{T_B}{2}(T_{n+1,m+1}-T_{n+1,m-1})\right\}\right]*(U_{n+1,m-1})+\left[\frac{S}{2}\cdot V_{n,m}\right]*(U_{n+1,m-1})-\left[\frac{P_{n+1,m}}{\Delta Z}\right]=+\left[\frac{4(1-N)}{Re^2}\{G\cdot Co_4+T_{n+1,m}(Co_5+Co_6T_{n+1,m})\}\right]+\left[\frac{4(1-N)}{Re\Delta Z^2}\cdot\{T_A+T_B(T_{n+1,m}-T_{n,m})\}\right]*(U_{n,m})-\left[\frac{2(1-N)\cdot U_{n-1,m}}{\Delta Z^2\cdot Re}\cdot T_A\right]-\left[\frac{P_{n,m}}{\Delta Z}\right]-\left[\frac{U^2_{n,m}}{\Delta Z}\right]-\left[\frac{S\cdot(1-N)}{\Delta Z\cdot Re}\cdot T_B\cdot(T_{n+1,m+1}-T_{n+1,m-1})\cdot(V_{n,m}-V_{n-1,m})\right] \quad (16)$$

where;

$$T_A=\left(Co_1+T_{n+1,m}(Co_2+Co_3T_{n+1,m})\right)$$

$$T_B=\left(Co_2+Co_3T_{n+1,m}\right)$$

$$\left[\frac{S^2(1-N)}{Re}\left\{T_A\frac{(2x-1)}{(x-1)}+T_B(T_{n+1,m+1}-T_{n+1,m-1})\right\}-\frac{S}{2}V_{n,m}\right]*(V_{n+1,m+1})+\left[\frac{2(1-N)}{Re}\left\{T_A\left(\frac{1}{\Delta Z^2}-\frac{S^2}{(x-1)^2}(2x^2-4x+3)\right)\right\}\right]*(V_{n+1,m})+\left[\frac{2(1-N)}{Re}\left\{\frac{T_B}{\Delta Z^2}(T_{n+1,m}-T_{n,m})-\frac{U_{n,m}}{\Delta Z}\right\}\right]*V_{n+1,m}+\left[\frac{S^2(1-N)}{Re}\left\{T_A\cdot\frac{(2x-3)}{(x-1)}-T_B(T_{n+1,m+1}-T_{n+1,m-1})\right\}+\frac{S}{2}\cdot V_{n,m}\right]*(V_{n+1,m-1})+\left[\frac{S}{12}\right]\cdot P_{n+1,m+2}-\left[\frac{2S}{3}\right]\cdot P_{n+1,m+1}+\left[\frac{2S}{3}\right]\cdot P_{n+1,m-1}-\left[\frac{S}{12}\right]\cdot P_{n+1,m-2}=\left[-\frac{U_{n,m}}{\Delta Z}\cdot V_{n,m}+\frac{4(1-N)}{Re\,\Delta Z^2}\cdot T_A\cdot V_{n,m}\right]+\left[\frac{2(1-N)}{Re\,\Delta Z^2}\cdot\left\{\frac{T_B}{2}\cdot(T_{n+1,m}-T_{n,m})-T_A\right\}\cdot V_{n-1,m}\right]-\left[\frac{S\cdot(1-N)}{Re\,\Delta Z}\cdot T_B\cdot(T_{n+1,m}-T_{n,m})\cdot(U_{n,m+1}-U_{n,m-1})\right] \quad (17)$$

Energy equation

$$\left[\frac{S}{2}\cdot V_{n,m}+\frac{S^2(1-N)}{\mathrm{Re}\cdot\mathrm{Pr}}\cdot\frac{(1-2x)}{(x-1)}\right]\cdot T_{n+1,m+1}+\left[\frac{U_{n,m}}{\Delta Z}+\frac{2(1-N)}{\mathrm{Re}\cdot\mathrm{Pr}}\cdot\left(2S^2-\frac{1}{\Delta Z^2}\right)\right]\cdot T_{n+1,m}+\left[\frac{S^2(1-N)}{\mathrm{Re}\cdot\mathrm{Pr}}\cdot\frac{(3-2x)}{(x-1)}-\frac{S}{2}\cdot V_{n,m}\right]\cdot T_{n+1,m-1}=\left[\left(U_{n,m}-\frac{4(1-N)}{\Delta Z\cdot\mathrm{Re}\cdot\mathrm{Pr}}\right)\cdot\frac{T_{n,m}}{\Delta Z}+\frac{2(1-N)}{\mathrm{Re}\cdot\mathrm{Pr}\cdot\Delta Z^2}\cdot T_{n-1,m}\right] \quad (18)$$

Integral continuity equation

$$\frac{3S^2(1-N^2)}{8}=\sum_{m=1}^{M}\left[(2m+F-1)U_{n+1,2m}\left(Co_4+\frac{Co_5}{G}T_{n+1,2m}+\frac{Co_6}{G}T^2{}_{n+1,2m}\right)\right]+\sum_{m=1}^{M-1}\left[(m+\frac{F}{2})\cdot U_{n+1,2m+1}\left(Co_4+\frac{Co_5}{G}T_{n+1,2m+1}+\frac{Co_6}{G}T^2{}_{n+1,2m+1}\right)\right] \quad (19)$$

The numerical calculations algorithm used is as follows:

Equation (18) for temperature was written for each radial position at first axial step. This gives a set of M-1 equations for unknowns T's that were solved by Gauss elimination method. Then equations (15-17) and with integral continuity equation (19) were similarly written and solved for the unknowns U,V and P and these gives (3M-2) equations for U,V and P unknowns. The known values of T, U, V and P were then used as input data to solve the next axial step.

The introduction of second derivative of velocity and temperature in the axial direction means that three axial positions were involved in the finite difference approximation, two positions (suffices "n-1" and "n") were known and one (suffices "n+1") was unknown. After solution of a given step, the old values at "n" and "n+1" become the new values at "n-1" and "n" respectively and old "n-1" data redundant.

Nusselt number

$$\mathrm{Nu}_z=\frac{2(1-\mathrm{N})\cdot\left(\frac{\partial \mathrm{T}}{\partial \mathrm{R}}\right)_1}{\mathrm{T}_{s_z}-\mathrm{T}_{b_z}} \quad (20)$$

EXPERIMENTAL APPARATS

The experimental apparatus, which has been designed and constructed to investigate combined convection heat transfer in an annulus where the outer cylinder is subjected to a constant heat flux while the inner cylinder is adiabatic. An open air circuit was used which included a blower (B), orifice plate section (C), settling chamber (D), test section and a flexible hose (E). The blower is driven electrically and the air flow rate can be regulated accurately by using a control The air induced by the blower, enters the settling chamber through a flexible hose (E). The settling chamber was carefully designed to reduce the flow fluctuation and to get a uniform flow at the test section entrance by using flow straightener (G). The air then passed through 1.2 m long test section. A symmetric flow and a uniform velocity profile produced by a well designed Teflon bell mouth (H) which is fitted at the annulus outer aluminum cylinder (I) and bolted inside the settling chamber (D). The inlet air temperature was measured by one thermocouple (J) located in the settling chamber (D) while the outlet bulk air temperature was measured by two thermocouples (Z) located in the test section exit as shown in **Fig.2**.

The test section consists of 4 mm wall thickness, 50 mm outside diameter and 1.2 m long aluminum cylinder (K) of inner cylinder located centrally in 5 mm thickness, 90 mm inside diameter and 1.2 m long aluminum of outer cylinder, by fitting it at the test section inlet with the 20 mm inside diameter, 50 mm

outside diameter and 15 mm long Teflon tube (N) and at the test section exit with the teflon piece (M). A ring (P) is used to hold and support the aluminum cylinder (K) with the teflon piece (N) centrally inside the settling chamber by adjustable screws (Q). The teflon was chosen because of its low thermal conductivity in order to reduce the heat loss from the aluminum cylinder ends.

The outer cylinder was heated electrically by using an electrical heater as shown in **Fig.3** section (A-A). The outer cylinder is covered by a 3 mm thickness asbestos layer (T), then a (2) mm in diameter nickel-chrome wire electrically isolated by ceramic beads (C) with diameter (6.5) mm, and then twenty layers of asbestos of thickness (25) mm to reduce the heat loss to minimum value. The temperature of outer cylinder was measured by fourteen asbestos sheath alumel-chromel (type K) thermocouples; there are three thermocouples (type K) on the outer surface of asbestos to calculate the conduction heat loss. The inner cylinder is insulated and it consists a teflon tube (S) and is covered by a 2 mm thickness asbestos layer (T), and the space between the asbestos and the inner cylinder wall is fitted with a fine grade sand (U) to avoid heat convection. The whole apparatus is designed with a view to obtain a good concentricity of the core cylinder and the containing cylinder. The measurements devices had been used including variac, digital voltmeter, clamp meter, two digitals thermometers.

RESULTS AND DISCUSSION

Theoretical results

Theoretical Results are studied mixed convection heat transfer to assisting and opposing air flow in a vertical annulus with adiabatic inner wall and uniformly heated outer wall. The ranges of governing parameters covered in the calculations are 400 $\leq$Re $\leq$ 2000, ($1.36\times10^5 \leq$ Ra $\leq 1.1\times10^7$), Pr=0.7 and N=0.555. The deviation in the average Nusselt number between the (12×48) grid sizes in r-z plane which has been used in all computations to a finer grid size (24×96) in r-z plane was found to be less than 0.5%. The temperature profile, velocity profile, variation of the outer tube surface temperature and local Nusselt number along the annulus has been investigated.

Temperature profile

The variation of temperature profiles along the vertical annulus is shown in **Fig.4** which are represented for Re = 1500 and heat flux q = 200 W/m^2, Ra=1.548×10^6. The figure shows a steep temperature gradient near the heated surface and the thickness of the thermal boundary layer gradually increases as the flow moves from annulus inlet towards annulus exit. It can be seen that there is a relatively high temperature variation near the heated surface causes an appreciable density change, which creates a rapid growth of thermal boundary layer along annulus length. **Fig.5** shows the effect of flow direction for various heat fluxes on the temperature profile at z = 0.72 m and Re=724. It can be seen that the temperature gradient with high heat flux is larger than that in low heat flux because of dominating natural convection. Also; it shows that the level of temperature profile with opposing flow is higher than that in aiding flow.

Velocity Profile

Development of the axial velocity profiles along the annulus axis in case of pure forced convection (i.e., buoyancy term is neglected), are shown in **Fig.6** for q $\approx$ 0 and Re =.724. Profiles reveal the limitation of the buoyancy effect and show approximately similar distribution about the middle of the annular space which is similar to pure forced convection behavior in agreement with **(Coney and El-Sharrawi 1975)**. The maximum axial velocity occurs at dimensionless radial distance ($r-r_i/r_o-r_i=0.5$). Figure shows also that the velocity increases with Re increasing because of the dominating pure forced convection in the heat transfer process.

Fig.7 shows the development of the axial velocity profiles for aiding and opposing flows at z = 0.72 m and Re=724 and for

various heat fluxes. It is clear from this figure that, when the free convection opposes the forced flow (i.e., for heating with down flow or cooling with up flow) the buoyancy force tends to retard the fluid near the heated boundary and accelerates it near the opposite adiabatic wall. In such case the maximum velocity profile distortion occurs when the slope of the profile at the heat transfer boundary reaches its minimum value. Therefore; in this case a possibility of flow reversal may occur near the heated wall if the natural convection is opposing the forced flow. On the other hand when the free convection aids the forced flow (i.e., upward flow) the fluid accelerates near the heated wall and decelerates near the opposite adiabatic boundary. But Fig.8 shows at z = 0.72 m and q = 1000 W/m^2 and various Reynolds number that the effect of forced convection is dominating with increasing Re. The velocities in aiding and opposing flows tend to approach to each other especially at the middle of annulus (at high Reynolds number).

Bulk Temperature

Fig.9 shows the variation of the bulk temperature (mixing cup temperature) with the axial distance z, corresponding to different heat flux and (Re =724) It is clear from this figure that the bulk temperature increases with increasing heat flux, the increase of local mixing causes an improvement in the local heat transfer process and reducing the heated surface temperature.

Surface Temperature

The outer cylinder surface temperature distribution along a vertical annulus is shown in **Fig.10** for constant heat flux (q = 700 W/m^2) and different Reynolds number (Re=400, 724, 1000, 1500, 2000). Figure shows that the outer tube surface temperature decreases as Reynolds number increases for the same heat flux.

Fig.11 shows the difference between aiding and opposing at the Reynolds number Re=724 and heat flux (370) W/m^2. It is clear from this figure that the outer tube surface temperature in case of opposing flow is higher than in aiding flow. This behavior can be attributed to that when the free convection aids the forced flow the density of the air near the wall decreases. The secondary flow assists main flow in removing heat from the outer tube surface and improving the heat transfer process because of the large velocity near the outer tube wall. On the other hand when the free convection opposes the forced flow, the velocities due to buoyancy flow and forced flow are in the opposite direction, in this case the buoyancy force tends to retard the fluid near the heated wall and accelerates it near the opposite adiabatic wall, so that the free convection effect will decrease in the case of the opposing flow causes the outer tube surface temperature distribution for opposing position to be higher than that for aiding position.

Local Nusselt Number (Nu_z)

The variation of local Nusselt number (Nu_z) with a logarithmic dimensionless axial distance (inverse Graetz number ZZ), is shown in **Fig.12**. The effect of heat flux variation (q=200, 370, 700, 1000, 1500) W/m^2 on the (Nu_z) along the dimensionless axial distance with constant Reynolds number (Re=1000). It is clear from this figure that the values of (Nu_z) is the same for different heat fluxes at the annulus entrance because of limitation of buoyancy effect at this region, then the values of (Nu_z) increases downstream as the heat flux increases. This behavior is due to the increase both thermal boundary layer thickness and the surface to bulk air temperature difference which accompanies with increasing the surface heat flux that accelerates the development of the secondary flow in the annulus down stream.

Fig.13 shows the effect of Reynolds numbers variation (400, 724, 1000, 1500, 2000) on the (Nu_z) along the dimensionless axial distance ZZ and constant heat flux (q=370 W/m^2). It is clear from this figure that the effect of secondary flow is small at the annulus entrance where the forced convection is dominant and the (Nu_z) values increase downstream of annulus as Reynolds number

decreases because of the dominant free convection.

Fig.14 shows the effect of aiding and opposing flow on the (Nu_z) values along the dimensionless axial distance ZZ for various values of heat transfer and constant Reynolds number (Re=724). It is clear from this figure that when the free convection aids the forced flow, the values of (Nu_z) are higher for the same logarithmic dimensionless axial distance (ZZ) than their corresponding values of the purely forced convection case ($q \approx 0$) and vice versa in the opposing direction. This is attributed to the higher velocities near the heated surface, and hence the decrease in the thickness of the developing boundary layer on that boundary, in case of an aiding free convection.

Experimental results

Surface temperature

The variations of surface temperature for different heat flux and Reynolds number equal to Re =1500 and for different Reynolds number and heat flux equal to 680 W/m^2 are shown in **Fig.15 & Fig.16;** respectively. **Fig.15** reveals that the outer surface temperature increases at the annulus entrance and attains a maximum value after which the surface temperature begins to decrease. The rate of surface temperature rises at early stage is directly proportional to the wall heat flux (422 to 980) W/m^2. The value of maximum temperature seems to move toward the annulus entrance as the heat flux increases. This can be attributed to the increasing of the thermal boundary layer faster due to buoyancy effect as the heat flux increases for the same Reynolds number. **Fig.16** shows the effect of Reynolds number variation (724, 1000) on the outer cylinder surface temperature. It is obvious that the increasing of Reynolds number reduces the surface temperature as heat flux kept constant.

Local Nusselt number (Nu_z)

The variation of the local Nusselt number with ZZ for Re=1500 and various heat flux is shown in **Fig.17**. It is clear from this figure that at higher heat flux, the value of local Nusselt number are higher than the results of lower heat flux. This may be attributed to the secondary flow superimposed on the forced flow effect increases as the heat flux increases that leading to higher heat transfer coefficient.

Verification of the results

Comparison with previous experimental

The experiments were done for heating outer tube annulus with radius ratio (0.555), (D_h=0.04 m), and (L/D_h=30) and air as a test fluid for present work. **Fig.18** reveals a comparison between the present experimental work for q=387 W/m^2 and Re=383 and the experimental work of (Falah 1993), who carried out it with internally heated inclined annulus of radius ratio (0.411), (D_h=0.043) and L/D_h=20.93, (q=283 W/m^2 and Re=300). It is clear from this figure that a convergence between the two curves is obtained.

Comparison with present theoretical results

Fig.19 shows a comparison between experimental and theoretical local Nusselt number in this work for Re=724 and q=370 W/m^2. Figure reveals that the experimental local Nusselt number follows the same trend and behavior as the present theoretical results but is approximately with means difference of 10.23 %.

Comparison with previous theoretical results

Fig.20 reveals a comparison between the local Nusselt number of the present work and the theoretical work of (Mohammed 2007), who carried out his work with internally heated vertical annulus of radius ratio (0.555), (Pr=0.72) and (q=95 W/m^2 , Re=500). It can be seen that the results have the same trend as that obtained in the present theoretical work.

CONCULUSIONS

The temperature profile along the annulus shows a steep profile near the heated

surface due to increasing of the thermal boundary thickness as the heat flux increases and decreasing of the Reynolds number at the same axial position, the increase in buoyancy effect causes an accelerate in the growth of the thermal boundary layer. Near the annulus entrance the velocity profiles for different heat flux were found to be similar to those for pure forced convection behavior. While the velocity profiles were distorted by the effect of the buoyancy force in downstream. The heat transfer process in the case of aiding flow is better than that in the case of opposing flow. The variation of the outer tube surface temperature along the annulus for both experimental and theoretical parts has the same trend and behavior. The buoyancy effect can be neglected at the annulus entrance for all Reynolds number and heat flux covered in this study. At constant Reynolds number the Nu_z value increases with increasing of the heat flux in the annulus downstream due to the increasing of buoyancy effect. At constant heat flux the Nu_z value increases at the annulus entrance as Reynolds number increases because of dominating forced convection, while the Nu_z value increases in the annulus downstream as the Reynolds number decreases due to free convection is dominant.

REFERENCES

Collins, "Combined convection in uniformly heated vertical pipe", Heat and mass transfer by combined forced and natural convection, (15th September 1971).

Coney J. E. R. and El-Shaarawi M. A. I. ,"Finite difference analysis for laminar flow heat transfer in concentric annuli with simultaneously developing hydrodynamic and thermal boundary layers " , Int. Journal for Numerical Method in Engineering, Vol. 9, pp. 17-38, 1975.

El-Shaarawi M. A. and Sarhan A., "Free convection effects on the developing laminar flow in vertical concentric annuli "J. Heat Transfer, Vol. 102, pp.617-622, November, 1980.

Falah A. Aboud, "Combined free and forced convection in an inclined Annulus"، M. Sc. Thesis, University of Basra, College of Engineering, Mechanical Department, 1993.

Hanzawa T., Sako A., Endo H., Kagwa M., Sunaga T**. and Koto K.,** "Combined free and forced laminar convective heat transfer from isothermally heated inner tube in vertical concentric annulus", J. Chemical Engineering of Japan ,Vol. 19 ,No. 1, pp. 78-81 , 1986.

Hashimoto K., Akino N., and Kawamura H., "Combined forced- free convection heat transfer to a highly heated gas in a vertical annulus" ،Int. J. Heat Mass Transfer, Vol.29, No.1, pp. 145-151, 1986.

Heggs and Ingham "Laminar flow combined in vertical annuli", Proceeding of the 8th Int. Heat Transfer Conference, Munchen, Fed. Rep.of Germany, Vol.2, pp. 941-956, 1988.

Kayes .W. M, "Advanced fluid dynamics and heat transfer"
Mc Graw-Hill, New York, (1966).

Mohammed. A. R. Nima, Developing laminar mixed convection heat transfer through concentric annuli" M. Sc. Thesis, University of Baghdad, College of Engineering, Mechanical Department, (2007).

Shaik Samivullah, "Laminar mixed convection in vertical channels" M. Sc. Thesis, King Fahd University of Petroleum and Minerals, Mechanical Engineering, 2005**.**

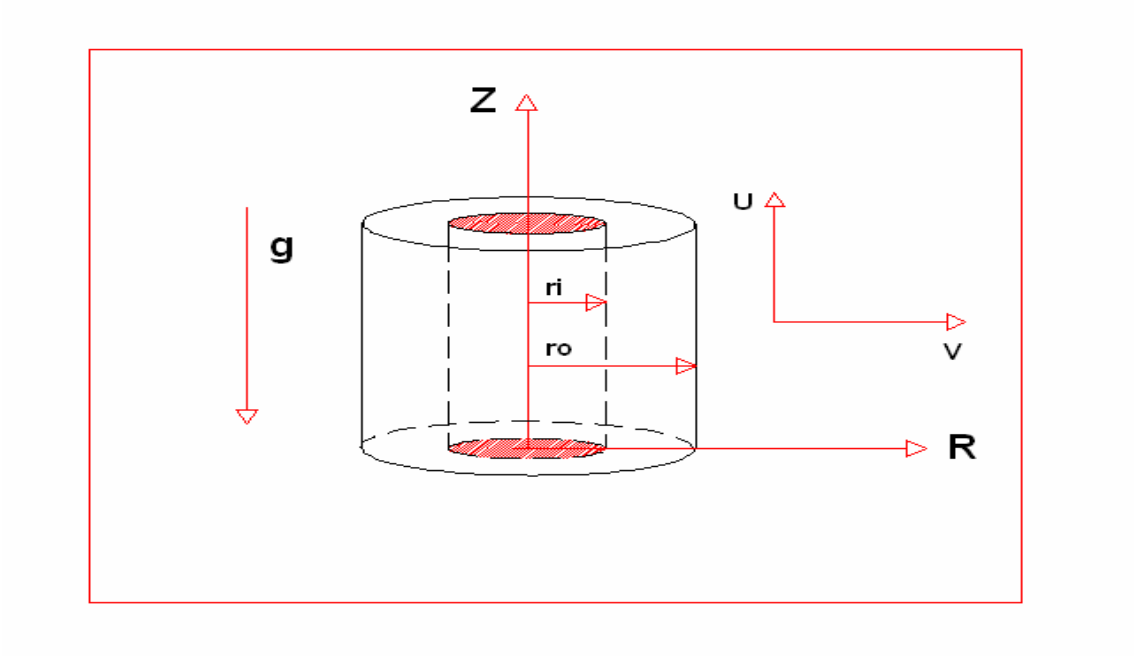

Fig. (1): Two- Dimensional Annular Geometry.

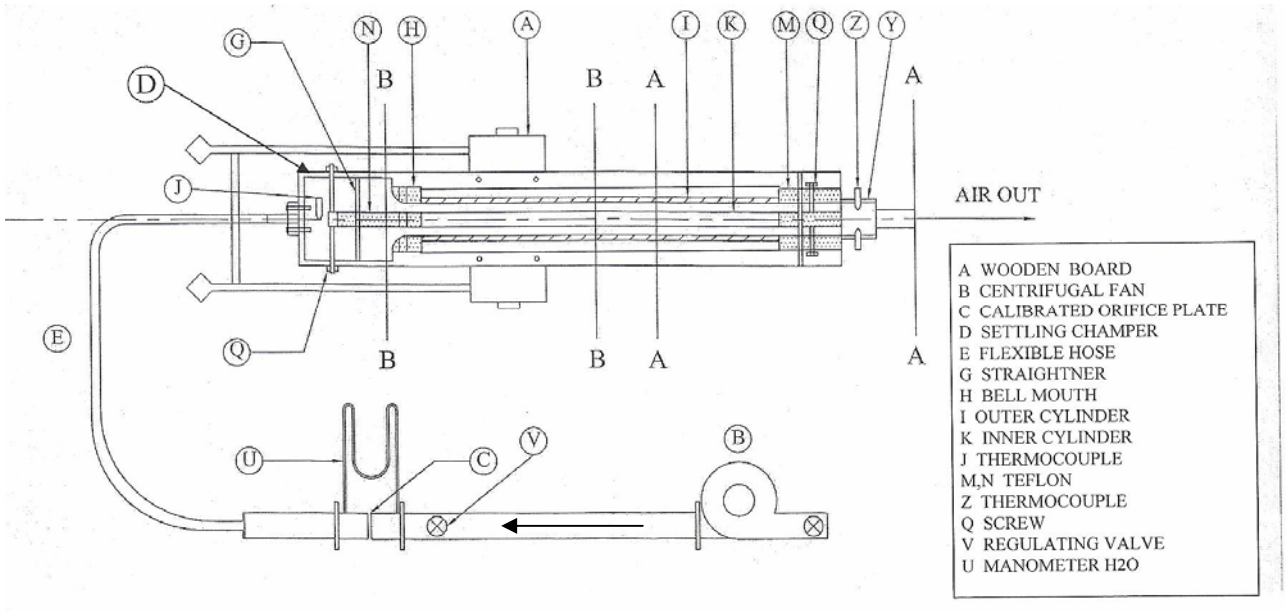

Fig. (2): Diagram of Experimental Apparatus.

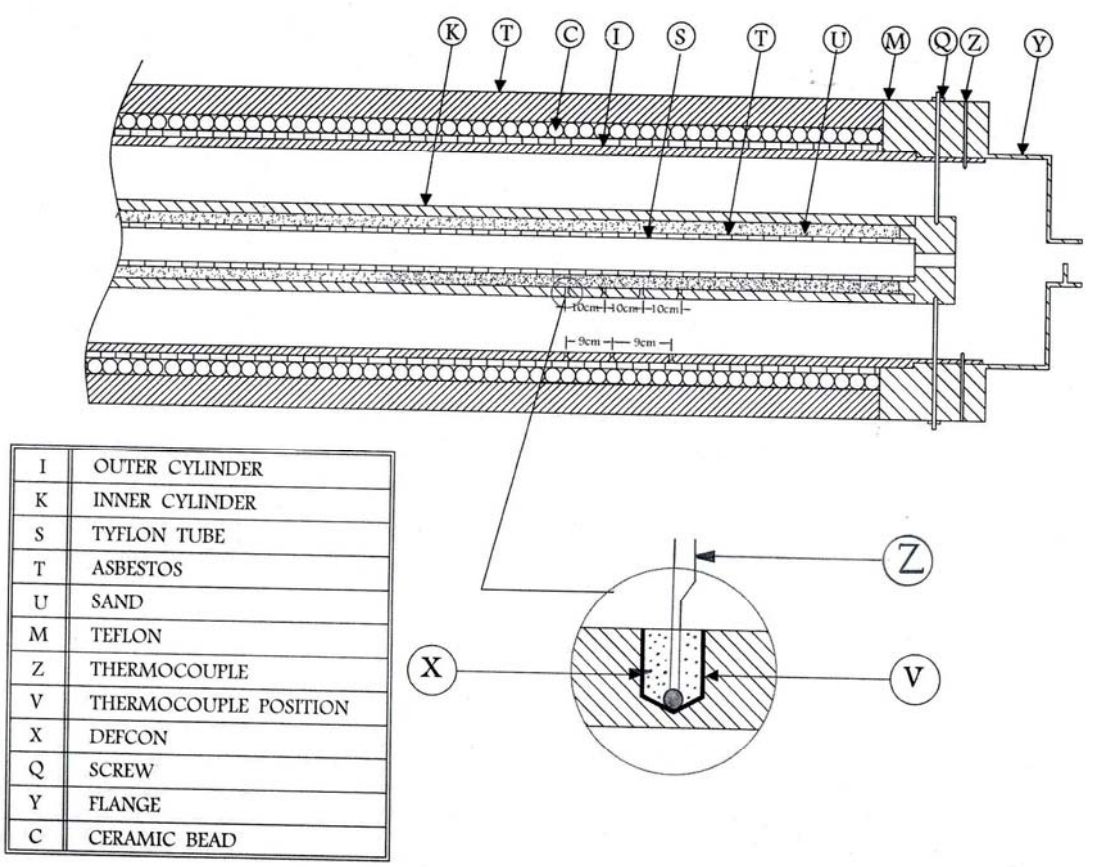

Fig. (3): Section A-A.

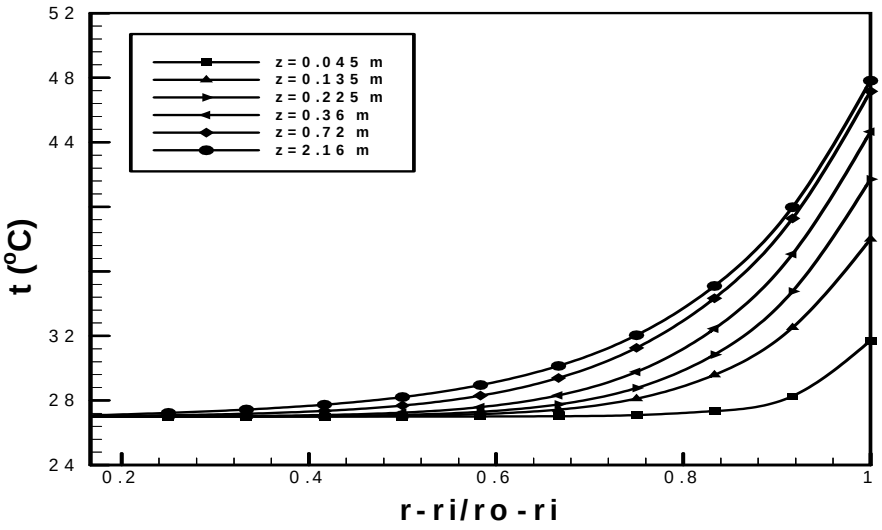

Fig. (4): Theoretical Development of the Temperature Profiles Along the Vertical Annulus for q=200 W/m^2, Re=1500 (aiding flow).

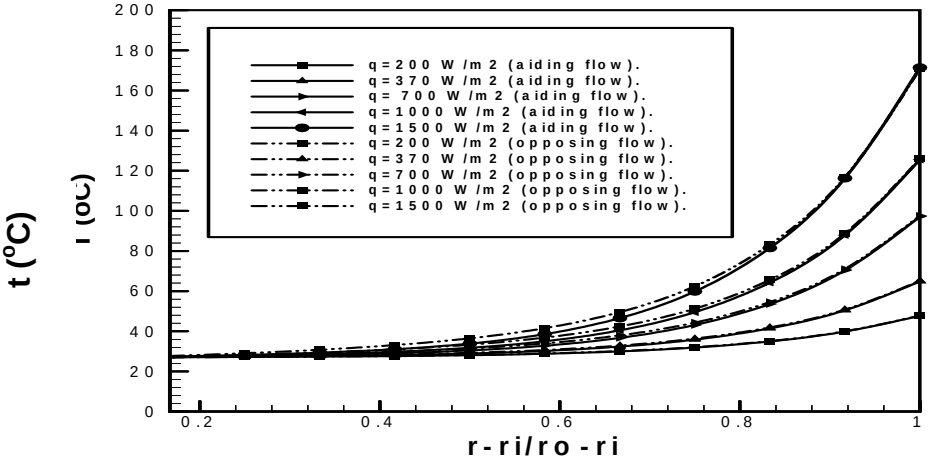

Fig. (5): Theoretical Development of the Temperature Profiles at (z = 0.72 m), Re=724 (aiding and opposing flow).

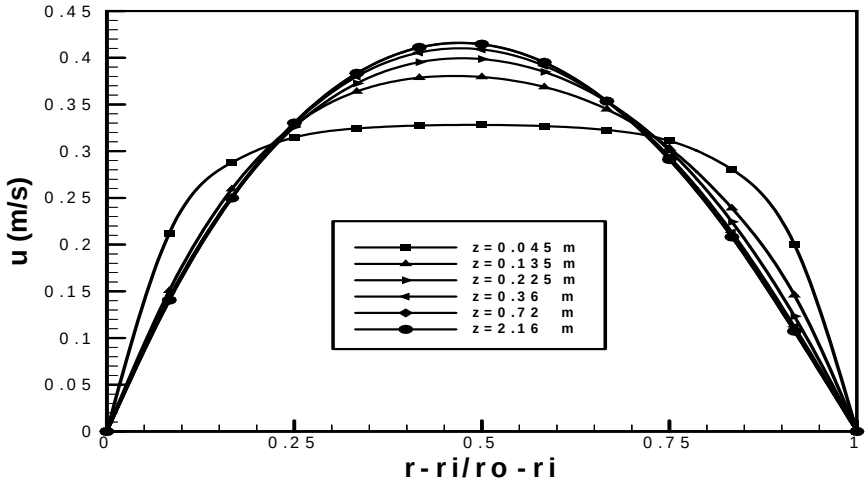

Fig. (6): Theoretical Development of the Axial Velocity Profiles Along the Vertical Annulus for q ≈ 0 W/m^2 , Re=724 (aiding flow).

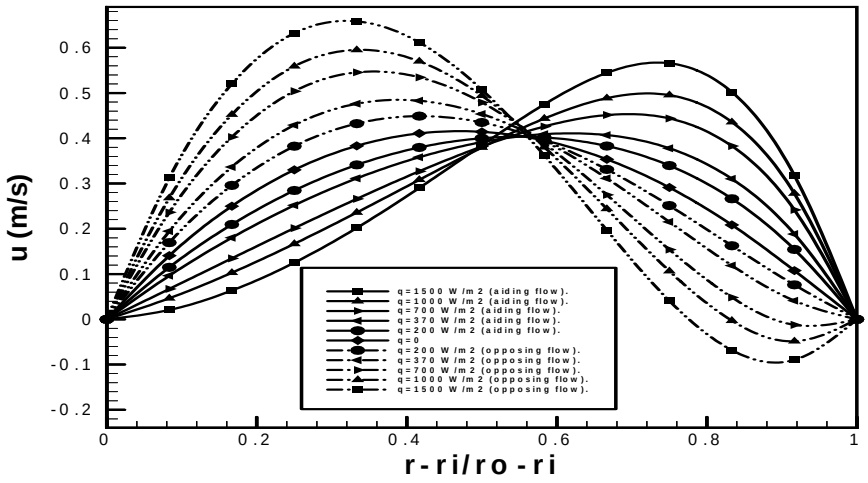

Fig. (7): Theoretical Development of the Axial Velocity Profiles at z =0.72 m, Re=724 for Various Values of q, (aiding and opposing flow).

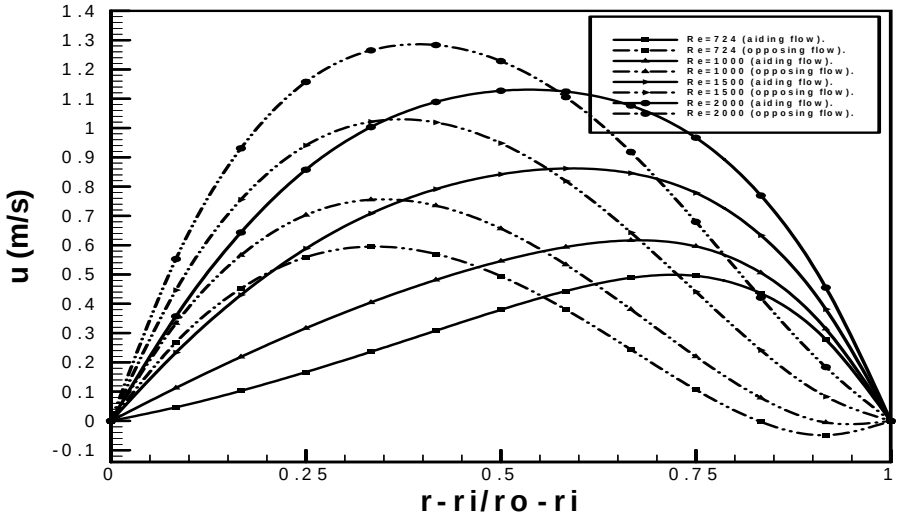

Fig. (8): Theoretical Development of the Axial Velocity Profiles at z =0.72 m, q = 1000 W/m^2 (aiding and opposing flow).

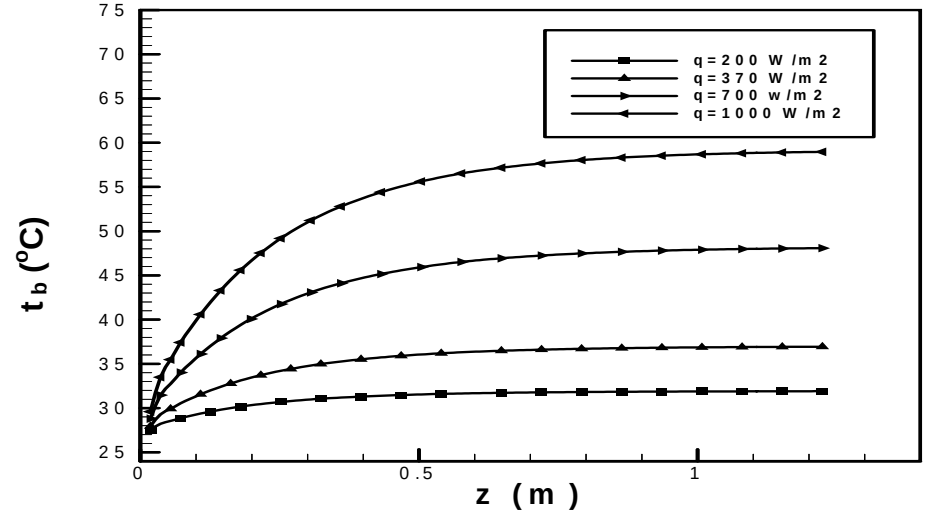

Fig. (9): Theoretical Variation of the Bulk Temperature Along the Axial Distance for Re=724.

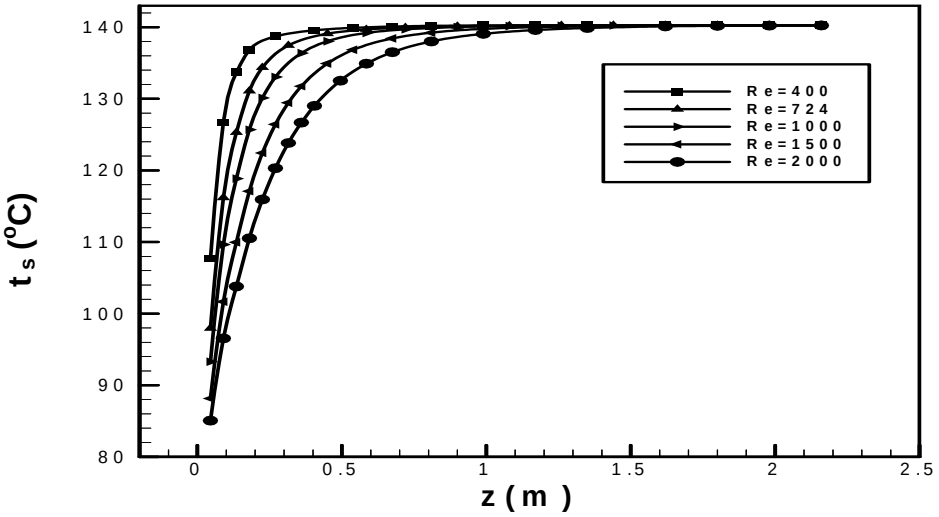

Fig. (10): Theoretical Variation of the Outer Tube Surface Temperature Along the Axial Distance for q =700 W/m^2.

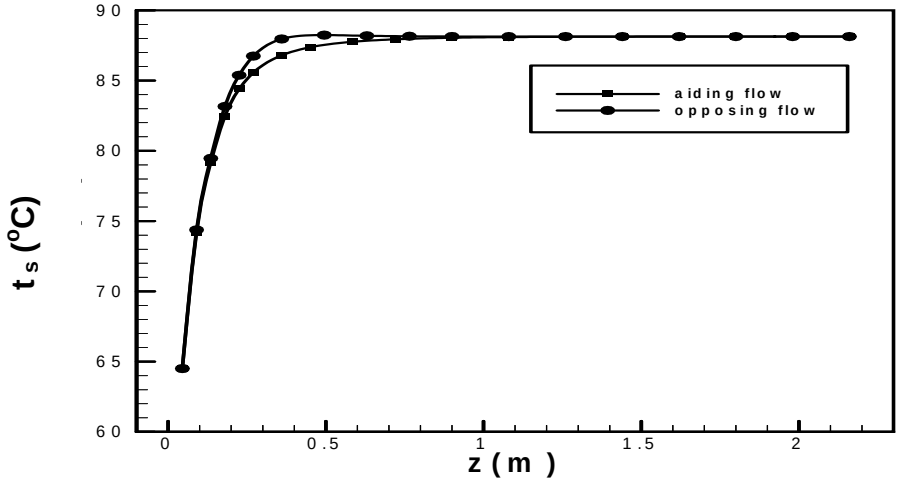

Fig. (11): Theoretical Variation of the Outer Tube Surface Temperature Along the Axial Distance for q =370 W/m^2, Re=724 (aiding and opposing).

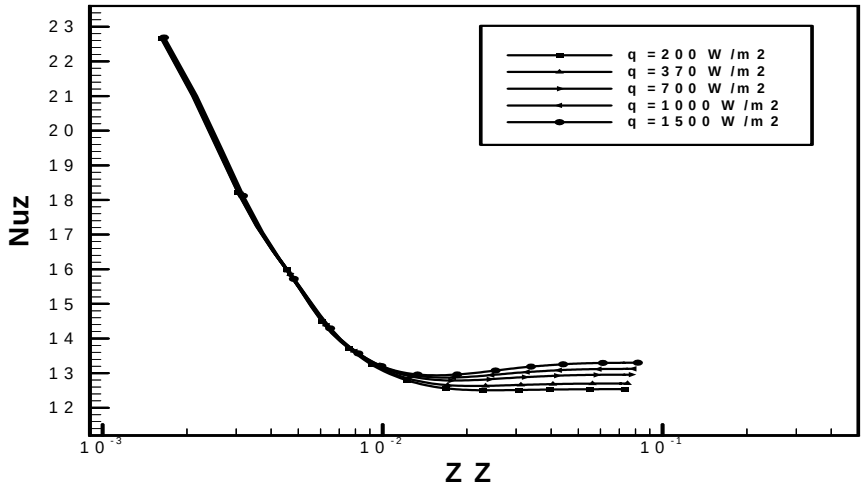

Fig. (12): Theoretical Local Nusselt Number Versus Dimensionless Axial Distance for Re=1000.

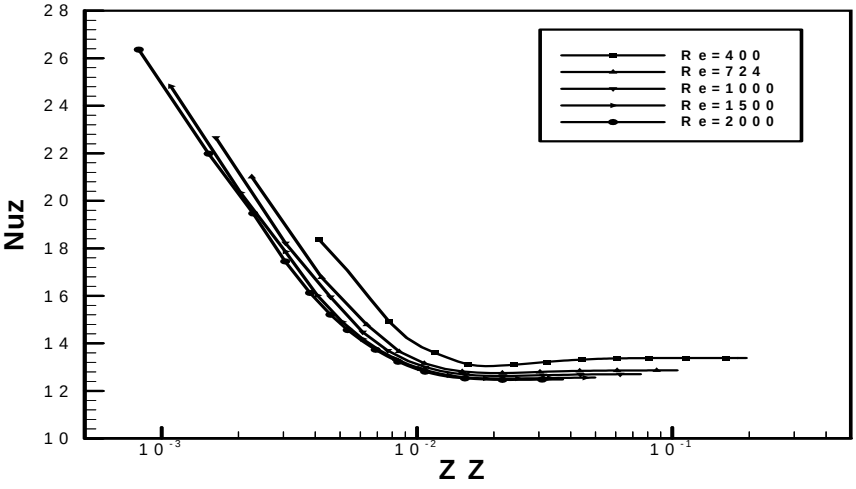

Fig. (13): Theoretical Local Nusselt Number Versus Dimensionless Axial Distance for q=370 W/m^2.

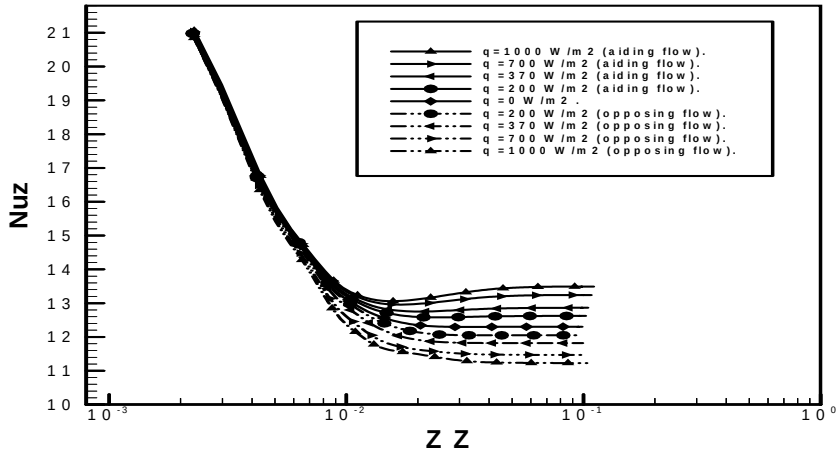

Fig.(14): Theoretical Local Nusselt Number Versus Dimensionless Axial Distance for Re=724 (aiding and opposing flow).

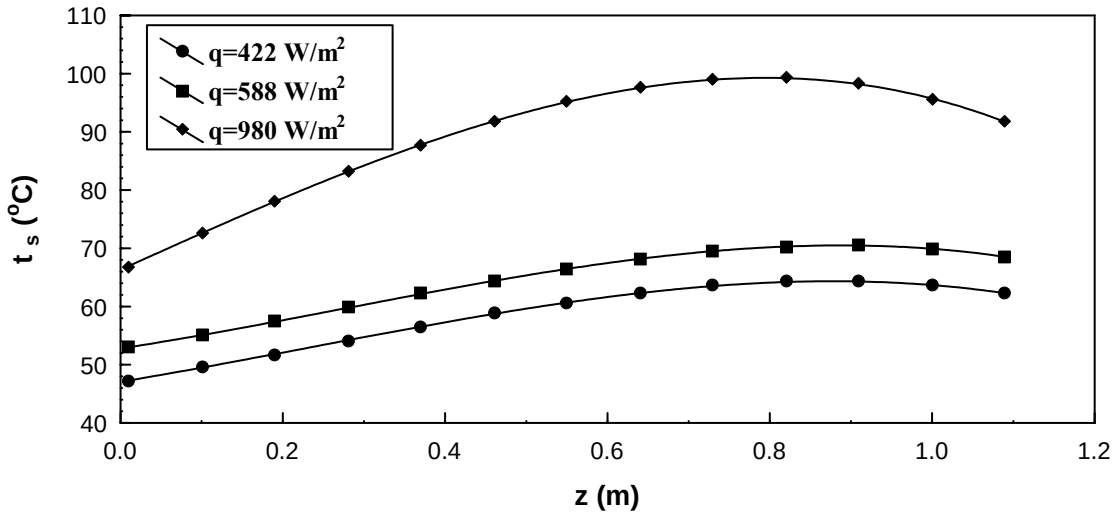

Fig.(15): Experimental Variation of the Surface Temperature with the Axial Distance, Re=1500.

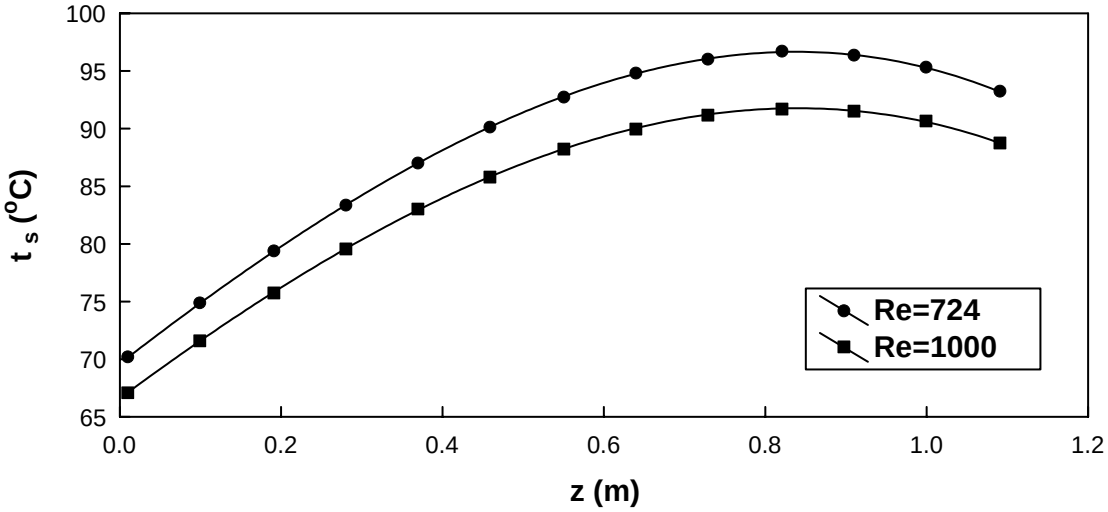

Fig. (16): Experimental Variation of the Surface Temperature with the Axial Distance, q=680 W/m^2.

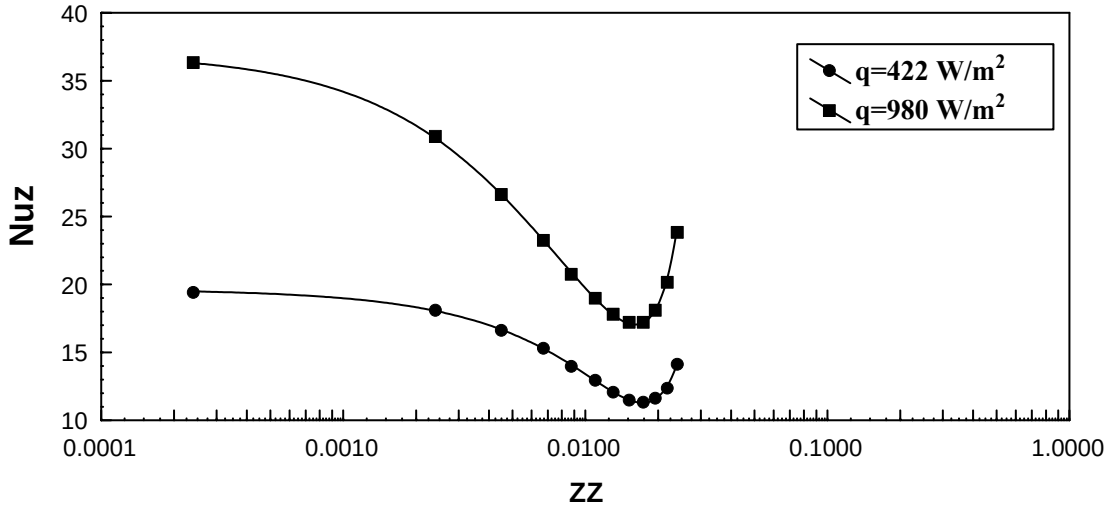

Fig. (17) Experimental Local Nusselt Number Versus Dimensionless Axial Distance, Re=1500.

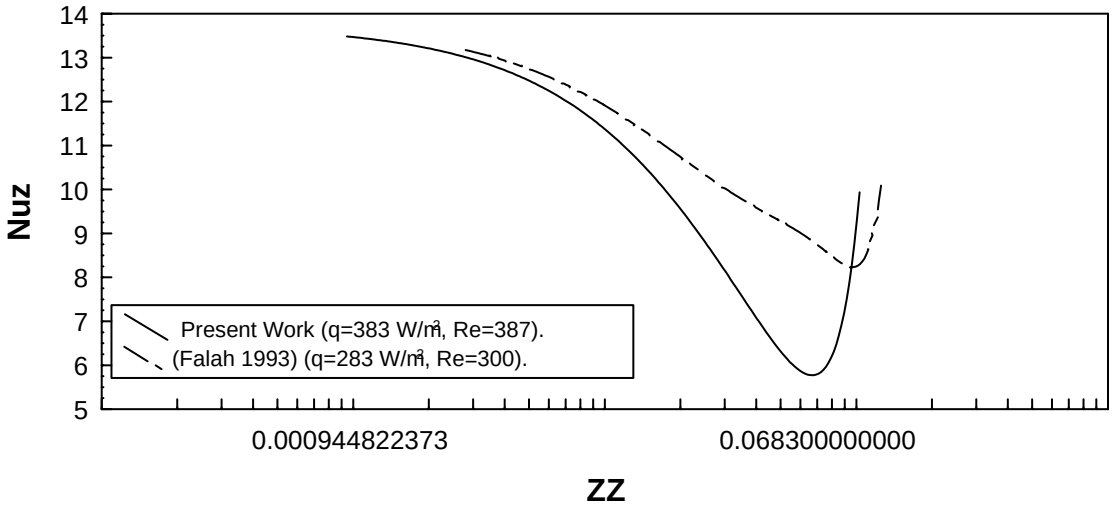

Fig.(18): Comparison of the Present Experimental Work with the Work of (Falah 1993).

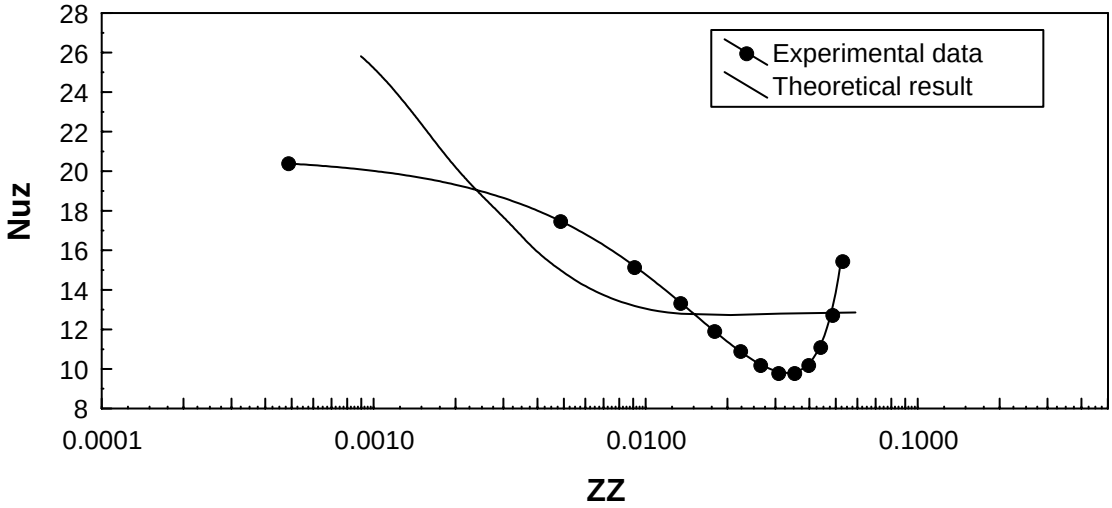

Fig.(19): Comparison of Experimental Nu_z with the Theoretical Result for Vertical Position, q=370 W/m^2 Re=724.

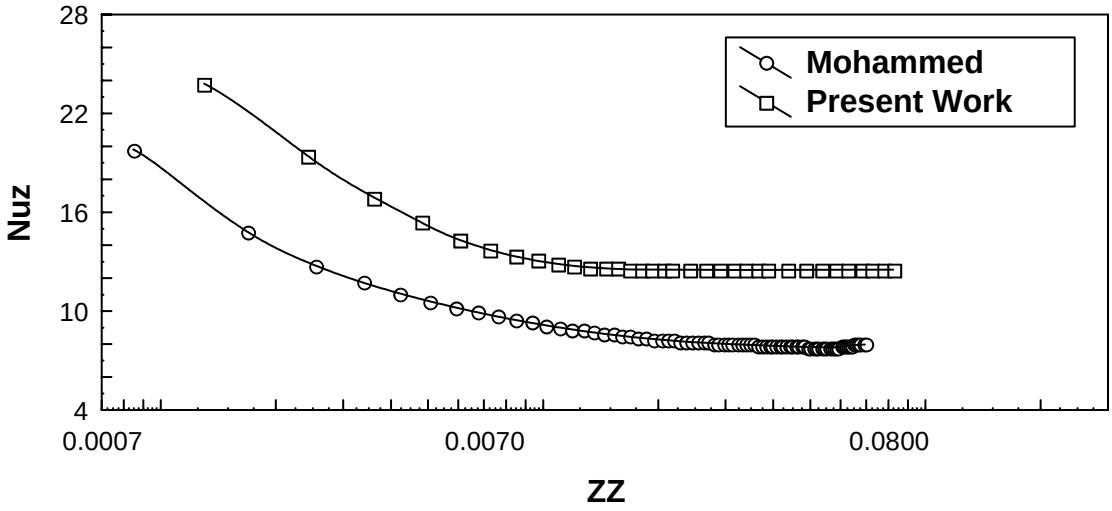

Fig. (20): Comparison of Theoretical Nu_z with the Theoretical Work of (Mohammed 2007) for Vertical Position, q=95 W/m^2, Re=500.

NOMENCLATURE
Symbols

$C_{1....}C_6$, Constants.
C_p, Specific heat at constant pressure.
D, Diameter
D_h= Hydraulic diameter= $2(r_o-r_i)$

$G = \frac{g r_o^{3}}{\nu_i^{2}}$ = Gravity acceleration

K, Thermal conductivity
M, Total radial mesh point
N, axial mesh point
N= Radius ratio=r_i/r_o

$P = \frac{p - p_i}{\rho u_i^{2}}$ = Pressure

q, Heat flux
r, Radial coordinate
r_i, Outer radius of inner cylinder
r_o, Inner radius of outer cylinder
t, Temperature
u, Axial velocity
v, Radial velocity
z , Axial coordinate

μ, Dynamic viscosity

υ, Kinematic viscosity

ρ, Density

ρ_i, Density at entrance

Nu, Nusselt number

$Pr = \frac{\mu \cdot Cp}{k}$ = Prandtl number

$R = \frac{r}{r_o}$ = Radial coordinate

$Re = \frac{u_i \cdot D_h}{\nu}$ = Reynolds number

$U = \frac{u}{u_i}$ = Axial velocity component

$V = \frac{v}{u_i}$ = Radial velocity component

$Z = \frac{z}{r_o}$ = Axial coordinate

ZZ = z/Re.Pr.D_h = Inverse Graetz number